Makara Journal of Technology

Volume 19 | Issue 3 Article 1

12-3-2015

# Independency of Elasticity on Residual Stress of Room Temperature Rolled Stainless Steel 304 Plates for Structure Materials

Parikin Parikin
*Center for Science and Technology of Advance Materials, National Nuclear Energy Agency, Banten 15314, Indonesia*, farihin@batan.go.id

David Allen
*School of Health and Mechanical Engineering, Queensland University of Technology, Brisbane QLD 4000, Australia*

Makara J. Technol. 19/3 (2015), 97-102
doi: 10.7454/mst.v19i3.3040

# Independency of Elasticity on Residual Stress of Room Temperature Rolled Stainless Steel 304 Plates for Structure Materials

Parikin[1*] and David Allen[2]

1. Center for Science and Technology of Advance Materials, National Nuclear Energy Agency, Banten 15314, Indonesia
2. School of Health and Mechanical Engineering, Queensland University of Technology, Brisbane QLD 4000, Australia

[*]*e-mail: farihin@batan.go.id*

## Abstract

Mechanical strengths of materials are widely expected in general constructions of any building. These properties depend on its formation (cold/hot forming) during fabrication. This research was carried out on cold-rolled stainless steel (SS) 304 plates, which were deformed to 0, 34, 84, and 152% reduction in thickness. The tests were conducted using Vickers method. Ultra micro indentation system (UMIS) 2000 was used to determine the mechanical properties of the material, i.e.: hardness, modulus elasticity, and residual stresses. The microstructures showed lengthening outcropping due to stress corrosion cracking for all specimens. It was found that the tensile residual stress in a specimen was maximum, reaching 442 MPa, for a sample reducing 34% in thickness and minimum; and about 10 MPa for a 196% sample. The quantities showed that the biggest residual stress caused lowering of the proportional limit of material in stress-strain curves. The proportional modulus elasticity varied between 187 GPa and of about 215 GPa and was free from residual stresses.

## Abstrak

**Independensi Elastisitas pada Tegangan Sisa Plat Baja Tahan Karat 304 Rol Temperatur Kamar untuk Bahan Struktur**. Kekuatan mekanik bahan secara umum sangat dibutuhkan pada setiap konstruksi bangunan apapun. Sifat mekanik bahan ini dapat diperoleh bergantung pada cara pembentukannya (dingin atau panas) selama fabrikasi. Telah dilakukan penelitian pada plat SS 304 rol dingin, yang dideformasi 0, 34, 84, dan 152% reduksi ketebalan. Pengujian dilakukan dengan metode Vickers menggunakan *ultra micro indentasi system* (UMIS) 2000 untuk menentukan sifat mekanik material yaitu: kekerasan, modulus elastisitas dan tegangan sisa. Struktur mikro untuk semua spesimen memperlihatkan lempengan memanjang akibat *stress corrosion cracking*. Hasil memperlihatkan bahwa tegangan sisa tarik pada spesimen maksimum; mencapai 442 MPa untuk sampel 34% reduksi ketebalan dan minimum; sekitar 10 MPa untuk sampel 196% reduksi. Kuantitas ini menunjukkan bahwa tegangan sisa terbesar mampu menurunkan batas proporsional bahan dalam kurva tegangan-regangan. Proporsional modulus elastisitas bervariasi sekitar antara 187 GPa dan 215 GPa dan nilainya tidak bergantung pada besaran tegangan sisa.

*Keywords: cold-rolling, hardness and microstructures, modulus elasticity, residual stress, stainless steel 304*

## 1. Introduction

Mechanical material properties are widely expected in general constructions of any building. The requirements of different shape and thickness in building construction materials leads to the convenience of easy installation of utility service. However, the presence of such fabrication processing may change the stress distribution within the materials, especially near surface regions. These internal stresses are called residual stresses. The stresses are defined as those stresses that would exist in elastic solid body if all external loads are removed [1]. The near surface residual stresses in engineering components can be introduced not only during fabrication (welding, forging, bending, and machining operations), but also as a result of deformation during use.

Severe accident analysis in a construction leads to assessment of the behaviour of mechanical and thermal responses of the material reactor (vessel, heat exchanger, etc.) and internal structures at higher temperatures. The case of an austenite to martensite phase transformation

[2] in SS 304 also occurs while rolled at below crystallization temperature that can significantly alter its structural, mechanical, and thermal material properties.

Dissimilar metal joints (welding) between austenitic stainless steels (SS-304) and carbon steels (SA-516) containing low amounts of carbon are extensively utilized in many high-temperature applications in energy conversion systems (heat exchanger). Higher temperatures, where increased creep strength and resistance to oxidation are required, are usually constructed with austenitic stainless steels [3]. The internal stresses around this metal joint might be very high, especially at heat affected zone (HAZ). It is prone to be attacked by corrosion.

The stainless steel type 304 [4], which is composed of (in weight percent) 0.06% C, 1.65% Mn, 0.33% Si, 0.005% S, 8.82% Ni, 17.72% Cr, and 0.40% Mo, has been a popular corrosion resistant material for the past 60 years. The research results of Huh et.al. [5] suggest that phosphate doped polyaniline coating on SS 304 is a strong candidate for corrosion protection of SS 304 in acidic chloride environments. The corrosion characteristic of the phosphate doped polyaniline films on SS resulted in not only dramatic increases in both corrosion potential and film breaking potential, but also large drop in corrosion current. In literature [6], it was reported that the best results were achieved when both the top and interfacial oxide layers were removed prior to the polymer deposition. The mechanism for corrosion protection was found to be anodic, i.e. the polyaniline film withdraws charge from the metal, passivating its surfaces against corrosion.

Among the important compositional modifications that improve corrosion resistance are (*i*) addition of molybdenum to improve pitting and crevice corrosion, (*ii*) lowering carbon content or stabilising with either titanium or columbium plus tantalum to reduce intergranular corrosion in welded materials, (*iii*) addition of nickel and chromium to improve high temperature oxidation resistance and strength, and (*iv*) addition of nickel to improve stress corrosion resistance. The equivalent composition of nickel-chromium in the 304 stainless steel illustrates that the alloying structure consists of austenite, martensite, and small amount of ferrite. These alloying elements commonly found in stainless steels are regarded either as austenite stabiliser (Ni) or ferrite stabilizer (Cr). The relative potency of each element is conveniently expressed in terms of either equivalence to nickel or chromium on a weight percent-age basis. The type 304 is the general purpose grade, widely used in applications requiring a good combination of corrosion resistance and formability [7]. This type yields higher strength on cold rolling. Cold Rolling processing of 304 stainless steels can yield martensitic transformation [2,8-9], $\gamma \rightarrow \alpha$ (austenite to martensite), which can cause a significant change in the mechanical properties of the material.

The study of microstructures is concerned essentially with the ability to distinguish between materials having different chemical composition, grain size, and orientation to distinguish between details separated by only small distances. Techniques for revealing microstructure features are almost all based either on the response of their details to incident radiation or on the quality and intensity of radiation emitted by features, when appropriately excited. The contrast of object is viewed as a bright and a dark field. Refraction effects on phase boundaries, for instance grain boundaries, may change the light path brightening part of the structure and darkening the neighbouring area. The intensity of this effect depends on the refractive indices. The surface micrographs of cold-rolled 304 stainless steel plates are also able to be analysed using the bright and the dark region, as a consequence of high and low intensity of light. However, there are many procedures relevant to measure microstructure and grain size. By using a microscope, the microscopy is reasonably accurate. The tendency of sizing statistically significant quantities of grains has led to the use of automatic image analysers.

In this paper the mechanical properties of specimens were measured using Hard Vickers Testing and a UMIS 2000 [10] nano-indentation system. Stiffness and hardness data of the specimens were obtained from representative stress-strain curves, loading-unloading of UMIS data measurements. The empirical curves were generated to show the residual stress effect on the mechanical properties of the specimens. Moreover, the micro-structures were observed using JEOL-35CF.

## 2. Experiments

Parts of this work-study have been carried out in Indonesia, while other works were performed in Australia. The type of SS-304 (JIS) standard sample was chosen to perform the experiments. The study consisted of analytical investigations of the structures of the 304 stainless steel plates, which had been rolled in room temperature with a reduction rate of 0.1 mm from about 1.25 cm to the common thickness of high tensile steels in cold working between about 0.05 cm and 1.01 cm. These correlated to the percentage of reduction of about 0%, 34%, 84%, 152%, 158%, 175%, and 196%, namely by R000, R034, R084, R152, R158, R175 and R196 respectively. The percentages were calculated by a formula:

$$\varepsilon(\%)=100\% \ln(T_o/T) \quad (1)$$

where $T_o$ is the initial thickness and $T$ is the thickness after rolling. This specification has been well introduced in optimum design of structures of sheets and railroad side ports, where higher physical properties are requested.

The study was also supported by observing the micro-structure. Microstructural topography was observed using JEOL-35CF scanning electron microscope at Physics Department QUT, Australia. The specimens were polished and etched using a mixed-solution of 30 mL HCl, 30 mL $HNO_3$, and 30 mL $H_2O$ at a heating temperature between of 70 °C to 80 °C for 2 minutes on a magnetic stirrer. This mixture is a strong acid solution to peel the surface, showing clearly the grain boundaries.

Indentation tests were carried out using both Vickers hardness testing and Ultra-Micro Indentation System - UMIS 2000. All instruments had been calibrated before used. The values of given hardness number were measured at the maximum depth and support the performed study. This mechanical property was basically dominated by the effect of nickel content in the 304 stainless steel, which could cause hardening when plastic deformation occurs [11], as a result of both strain hardening and strain induced transformation.

The Vickers hardness test results provide very interesting information. The principle of this test was based on an indenter of definite shape that was pressed into the test material under a specified load, and the diagonals of the indentation were measured. The hardness number was then calculated by dividing the load by the surface area of the impression. In this case, the indenter was a square-based diamond pyramid with an inclined angle of 136°. This was because of it approximated the most desirable ratio of indentation diameter to spherical diameter, which was used in ultramicrohardness. This diamond indenter was well suited to measuring the hardest material up to VHN 1500. The Vickers hardness number was obtained from the ratio of the applied load to the surface area of the indentation as in the following formula:

$$VHN(Kg/mm^2)=1.854P/d^2 \quad (2)$$

where $P$ is applied load mass (Kg), and $d$ is mean diagonal of indentation measured (mm).

In microindentation test, a force driven micro-mechanical probe with a spherical diamond indent or having nominal radius of 50 μm was utilized. The true equivalent radius over depth penetration was obtained by applying the expected compliance for standard stainless steel of known properties and a tip radius file generated by applying the formulated mechanics of deformation for spherical contact on a solid. Indentations were performed with depth datum at contact force of 0.1 mN. A maximum indenting force of 50 mN was used in all cases. The indentation force was systematically varied in a load-partial unload cycle over 20 steps, and in each case indentation depth was recorded automatically. The elastic-plastic analyses were carried out using the associated computer package, which was based on classical indentation mechanics of spherical tipped indentors. Specimens were mounted by superglue on the magnetic sub-based supplied with the UMIS 2000. For every specimen, total 11 indentations were made, and the closest 9 were averaged for final determination of mechanical properties. The empirical curves were then developed, and the large data were collected and stored in a computer.

## 3. Results and Discussion

**Microstructures**. The inspection of the microstructures was performed by using JEOL 35CF SEM, because the larger depth of field in the instrument was a distinct advantage. Especially, since it could show the contrast of surface topography. The grain sizes or localized attack due to stress corrosion cracking on the specimens could clearly be observed. The stresses were a form of failure induced by the conjoint action of tensile stresses and particular types of corrosive environments. The stresses were either residual or cracking take place in a direction normal to the compressive stresses, often at stress level below the yield strength of the material. The crack propagation mechanisms have been theorized based on anodic dissolution at the crack tip, passivation at the point prevented by plastic deformation [7]. The principal role of plastic deformation was to accelerate the dissolution process, where hydrogen ions in the surface rapidly captured a free electron to become hydrogen atom. The atom, then, migrated to the crack tip where it was absorbed within the metal lattice, causing mechanical rupture. This extends the crack, and further anodic dissolution then occurred on the newly exposed surfaces. These features can be seen in Figure 1.

The figure indicates the surface micrographs of some specimens used in the experiment, taken from transverse section of plate thickness or perpendicular to rolling direction. The increases in martensite volume fraction can clearly be observed from etching attacks on the surfaces. The interconnected grains as described above were exhibited from the occurrence of outcropping inclusions become longer in size as the percent reduction increased. It was revealed by the presence of elongated particles or clusters of second phases (martensite) in the form of plastic inclusions. These inclusions appeared to dissolve quickly, creating long narrow passages from the end faces into the body of specimens. These passages did not provide ready access for the ingress of the new acid, and it was thought that this gave rise to the formation and concentration of hexavalent $Cr^{+6}$ ions [12]. This led to particularly aggressive corrosion conditions within the passages and intergranular attack proceeded very quickly along the adjacent grain boundaries. The effect is known as end-grain attack, and it can lead to weight losses far in excess of experienced in cleaner steels or those containing shorter inclusion.

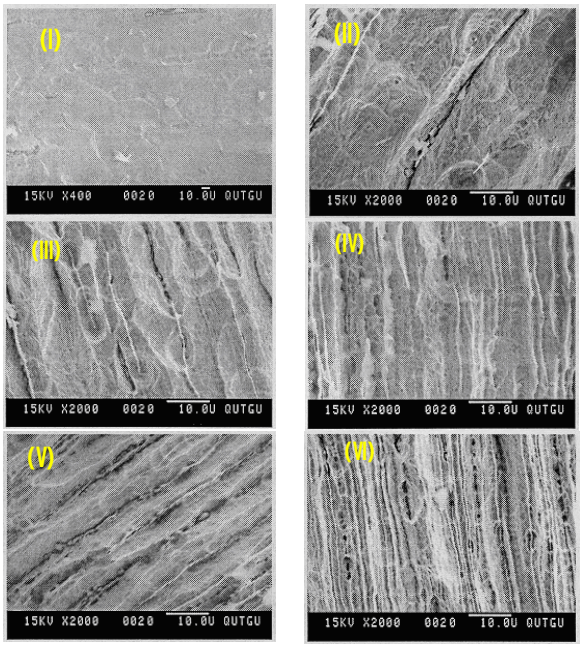


**Figure 1. End Grain Attacks from Outcropping Inclusions; Elongated Inclusions Outcropping on Transverse Sections (Perpendicular to the Rolling Directions) on (I) R000, (II) R034, (III) R084, (IV) R152, (V) R175 and (VI) R196 Dissolved in Nitric Acid, Chloride Acid and Water in Balanced Fraction. Magnification: 400x and 2000x**

**Hardness**. The measured VHN is illustrated in Figure 2 and listed in Table 1. The figure shows an increase of Vickers hardness number as reduction in thickness increasingly larger. The values were strongly affected by both strain hardening and the formation of martensite in the surface specimens. The martensite phase was found to be denser than austenite phase. The empirical prediction indicated that the more cold reductions, the more martensite formation and the harder the materials (shown in Figure 2).

**Stress-strain curves**. Figure 3 shows the force displacement data obtained for R000, R034, R084, and R152 specimens. All of the specimens exhibited significant plastic deformation even at relatively low load where the unload data points deviated from the loading curves. Meanwhile, Figure 4 shows the variation of elastic modulus *E* with percent reduction for the inspected specimens. The value of E (listed in Table 2) settled to reduce from 187 GPa, when the residual stresses remained in the specimens. The values of stiffness decreased significantly as the residual stresses achieved the higher values. This matched the known elastic lattice properties of the stainless steel specimens, which have been analyzed in X-ray diffraction technique and Rietveld method [13-14]. It is shown as the maximum residual stress remained in the specimens, the stiffness tended to reach a minimum value. The stiffness approximately healed to initial condition as the residual stress decreased, leaving the material.

Analysis of the raw data can be represented on a stress-strain curve. Here, the indentation stress (hardness) was compiled from the ratio of indentation force to the area of the circle of contact. The strain was a representative strain, which is the ratio of the radii of the contact circle and that of the indenter. Its relationship with the true strain was independent on the Poisson's ratio and the geometry of the tip. However, a fairly generalized value for the true strain has been estimated [10] to be about 0.2ε for a spherical tip indenter.

Figure 5 shows a typical curve obtained for all of the specimens. This curve was analogous (but not equivalent) to stress-strain curves obtained in a conventional uni-axial test. Again, the hardness at yield here did not exactly correspond to the true yield value.

The relationship between the contact pressure and the true yield value depended on a constrain factor determined by the amount of elastic region beneath the plastic deformation. For very ductile metal such the stainless steel, a constrain factor of 3 was adequate.

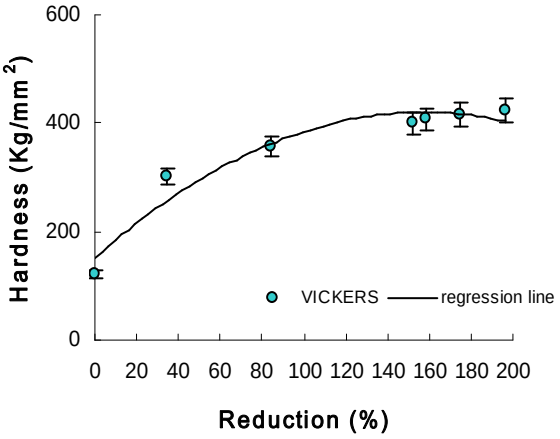


**Figure 2. Hardness Properties of Cold-rolled 304 Stainless Steel Specimens Measured by Vickers Hardness Test**

**Tabel 1. Hardness of un/-rolled Specimens**

| Specimens | Thickness Reduction (%) | Hardness (kg/mm$^2$) |
|---|---|---|
| R000 | Unrolled | 122 |
| R034 | 34 | 303 |
| R084 | 84 | 356 |
| R152 | 152 | 404 |
| R158 | 158 | 407 |
| R175 | 175 | 416 |
| R196 | 196 | 424 |

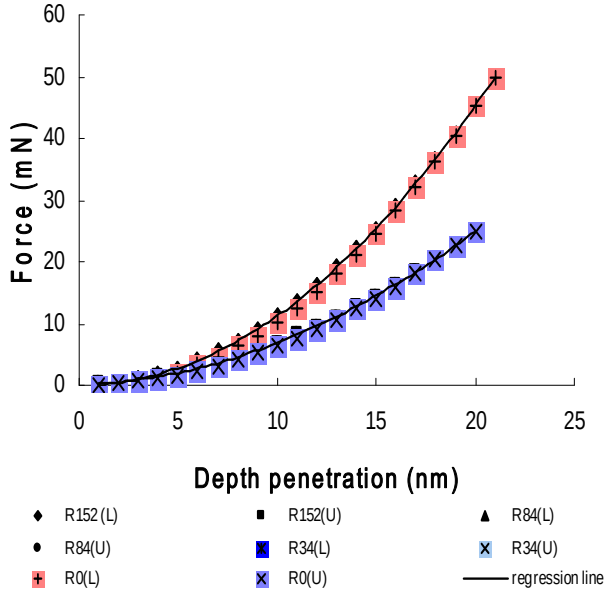


**Figure 3. Force Displacement Curve Obtained for All of Tested Specimens**

**Tabel 2. Modulus Elasticity of un/-rolled Specimens**

| Specimens | Thickness Reduction (%) | Modulus (GPa) |
|---|---|---|
| R000 | Unrolled | 187.00 |
| R034 | 34 | 147.85 |
| R084 | 84 | 162.42 |
| R152 | 152 | 171.23 |

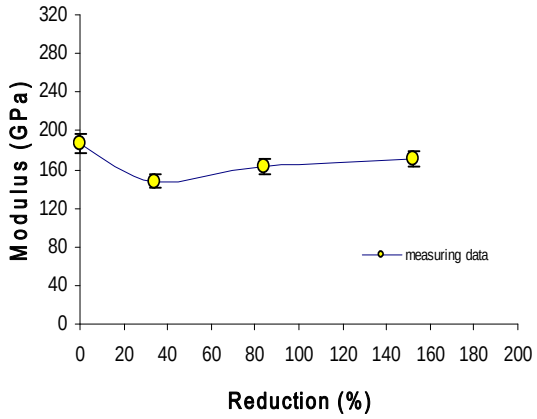


**Figure 4. Modulus Elasticity of R000, R034, R084, and R152 Specimens**

The distinctly visible influences of the residual stresses caused yielding earlier than was assumed if they were ignored. This feature was displayed in R000 specimen. They caused reduction in the stiffness of the specimens (see Figure 4). As shown in Figure 5, although the effect of the residual stresses was relatively not very essential, the residual stresses, nevertheless, lower the proportional

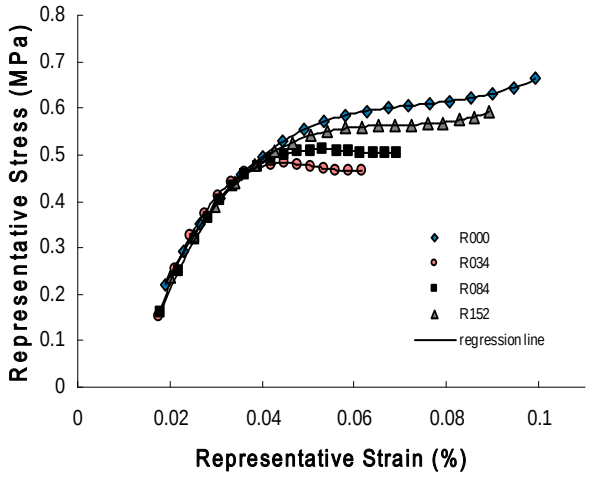


**Figure 5. Representative Stress Strain Curve Showing Effect of Residual Stresses on the Proportional Limit. It Shows the Residual Stresses caused Yielding Earlier**

limit. The measurements demonstrated how the residual stresses contributed to the stress-strain curves. It was complicated to estimate precisely how far the proportional limit reduced, owing to this information was only an analogous of the true stress-strain curves. However, the illustrated pictures are able to represent the effect of the residual stresses in the material. The information strongly supports an assumption that the elastic behaviour of the material cannot be predicted correctly without consideration of the residual stresses [15].

## 4. Conclusions

The microstructures indicated that the increases in martensite volume fraction were clearly observed from etching attacks on the surfaces. The interconnected grains were exhibited from the occurrence of outcropping inclusions and become lengthening as the percent reduction increases. The presence of elongated particles or clusters of second phases (martensite) in the form of plastic inclusions was apparent. These inclusions revealed to rapidly dissolve, forming long narrow passages from the end faces into the body of specimens.

Cold rolling caused an increase in hardness of material, whereas the mechanical properties measured from the value of modulus of elasticity *E*, decreased from 187 GPa, when the residual stresses remained in the specimens. The values of stiffness reduced significantly as the residual stresses reached the highest values (R034). As the maximum residual stress (442 MPa) remained in the specimen, the stiffness tended to have a minimum value. The stiffness approximately healed to initial condition as the residual stress left the material. The effect of the residual stresses was relatively not very essential; the residual stresses, however, lowered

the proportional limit. Estimating precisely how far the proportional limit reduced was very complicated because the UMIS 2000 information was only an analogous of the true stress-strain curves. Nevertheless, the illustrated information was representatively telling about the effect of the residual stresses in the material. This information strongly supported an assumption that the elastic behaviour of the material cannot be predicted correctly without consideration of the residual stresses.

## Acknowledgements

The writer would like to express his thanks to Prof. Dr. John Bell, Dr. Ayo Olofinjana from Queensland University of Technology, Drs. Agus Hadi Ismoyo, M.T. for their kindness and helpful. Also, I wish to thank to BPPT committee for financial supports of STAID-LINK.

## References

[1] Parikin, P. Killen, A. Rafterry, Atom Indonesia J. 35/1 (2009) 19.
[2] S. Rajasekhara, P.J. Ferreira, Acta Mater. 59 (2011) 738.
[3] M. Saini, N. Arora, C. Pandey, H. Mehdi, IJRET. 3 (2014) 2321.
[4] C. Stainless, Stainless Steel 304/04L Technical Data, *http://www.conexstainless.com/ technical-specification/-STAINLESS-STEEL-304-GRADE-SS-304-.html*, 2015.
[5] J.H. Huh, E.J. Oh, J.H. Cho, Synthetic Metals. 153/21 (2005) 13.
[6] A.A. Hermas, M.A. Salama, S.S. Al-Juaida, A.H. Qusti, M.Y. Abdelaal, Prog. Org. Coat. 77/2 (2014) 403.
[7] C. Cortiga, O. Bologna, C. Deac, Acta Universitatis Cibiniensis–Technical Series. LXIV/1 (2014) 28.
[8] H.K. Yeddu, A. Borgenstam, P. Hedström, J. Ågren, Mater. Sci. Eng. A 538 (2012) 173.
[9] M. Tajally, E. Emadoddin, Mater. Des. 32/3 (2011) 1594.
[10] V.I. Levitas, J. Mc.Collum, M. Pantoya, N. Tamura, J. App. Phys. 118/9 (2015) 94.
[11] J.M. Lackner, L. Major, M. Kot, Bull. Polish Acad. Sci. Tech. Sci. 59/3 (2011) 343.
[12] V.I. Levitas, M. Javanbacht, J. Mech. Phys. Solids. 82 (2015) 345.
[13] R. Naraghi, P. Hedström, A. Borgenstam, Steel Res. Int. 82 (2011) 337.
[14] Parikin, Bandriyana, I. Wahyono, A.H. Ismoyo, Atom Indonesia J. 39/2 (2013) 65.
[15] M. Sharma, A. Kumar, IJCSCE Special Issue on Recent Advances in Engineering & Technology NCRAET. 5/1 (2013) 13.